Feb. 1995

LU TP 95-3

Final State Interactions in the (Nuclear) FRITIOF String Interaction Scenario

B. Andersson[1], A. Tai [2] and Ben-Hao Sa [3]

Department of Theoretical Physics
University of Lund
Sölvegatan 14A
S-223 62 Lund, Sweden

FAX 46 46 104438

To be published in **Z. Phys. C Particles and Fields**

Abstract

We consider the final state reinteraction of the produced hadrons in a scenario with the initial high energy nuclear interaction provided by the FRITIOF Model. The basic idea is that any produced hadron is able to reinteract in accordance with the known cross sections (using classical trajectories for the motion and an impact parameter description of the interaction) from the Landau-Pomeranchuk formation time and onwards. This is treated as a rescattering transport process included in a Monte Carlo simulation subroutine, LUCIAE, to be connected to the FRITIOF, the ARIADNE, PYTHIA and the JETSET programs. We include a set of predictions, in particular on strangeness production, from the ensuing model.

[1]bo@thep.lu.se, Tel. 46 46 109079

[2]taian@thep.lu.se, Tel. 46 46 103496

[3]Permanent address: China Institute of Atomic Energy, P.O.Box 275, Beijing,102413 China. E-mail address:sabeah@bepc2.ihep.ac.cn

1 Introduction

In high energy heavy ion interactions there is a large amount of final state particles produced (mostly in the centre of phase space) and also a large nucleon density (in particular from the spectator nucleons in the nuclear fragmentation regions). It is then conceivable that there will be reinteractions due to this large hadronic density. In this paper we will with minimal (new) dynamical input introduce such a rescattering process for the model FRITIOF, [1][2].

FRITIOF is a model for inelastic hadron-hadron scattering and it has been successful in describing many experimental data from low energies via the ISR-regime and all the way to the top SPS energies, [2]. It has later been extended to hadron-nucleus and nucleus-nucleus collisions by the use of of superpositions of binary hadron-hadron collisions and simple geometry. This means an impact parameter description of the interaction between the impinging projectile(s) and the nucleus treated as a "frozen" bag of nucleons. (Any timescale for the changes of the nuclear state is much longer than the interaction times between the nucleons). Lorentz contraction means that the projectile(s) tend to hit many nucleons almost simultaneously, which leads to the large final state densities mentioned above.

FRITIOF was originally conceived as a string-dynamical hadronic interaction model, without color exchange. It is endowed with a simple longitudinal energy momentum exchange mechanism, leading to highly excited final state strings. These are afterwards fragmented in accordance with the Lund Model, in particular using the JETSET, [3], Monte Carlo routines. It has been extended for large energies to Rutherford parton scattering and also contains gluonic bremsstrahlung, using the Lund Dipole Cascade Model (DCM), [4], and (due to the expected extensions of the emitters) a softening mechanism, described by the Soft Radiation Model (SRM), [5]. This is implemented (for the Rutherfords) by PYTHIA, [6], and for the DCM and SRM by ARIADNE, [7]. The above-mentioned features of FRITIOF are described in section 2.

It is well-known that there is a shortest timescale before it is possible to differ between the excited hadronic state per se and its final state particle components. We will for that purpose make use of the notion of *the Landau-Pomeranchuk formation time.* We consider the formation time concept briefly inside the Lund String Fragmentation Model and also present the considerations behind our initiation in space-time of the final state particle distributions in section 3.

The basic idea for the rescattering process is that any hadron after its formation time may reinteract with any other hadron "along" its orbit, which we describe in terms of (relativistical) classical mechanics. In section 4 we describe the way these interactions are implemented into the model and also the considerations behind the particular choice of subprocesses which are included.

The rescattering effects were noticed many years ago. The study by J. Ranft [8]shows that for secondary particles produced in hadron-nucleus collisions with rapidities below y≈2 in the target rest frame, the model predictions without rescattering were found to be too low compared with data. So far the rescattering effects have been studied by a few authors [9][10][11] and have been implemented in MCFM, RQMD and QGSM. There are a few features in common in all these studies although the details of the ansatz used in different models are not the same: it is well accepted that the concept of formation time plays a crucial role in the rescattering and the rescattering tends to enhance the produced transverse energy, the particle production, mean transverse momenta and strangeness production. The formation time in those models is a parameter determined by comparing model predictions with experimental data and a mean value of the formation time is found to be about 1 fm/c in the rest frame of the rescattering object (string, quark, diquark or hadron) in all models. We will in this paper present our approach to the rescattering inside the framework of FRITIOF model and the approach is just a natural generalization of Lund String Fragmentation Model in nuclear matter.

It is evident that there is a very wide range of possible final state interaction channels. Some of those channels are significant in the sense that they provide new observable content to the model, eg strangeness enhancement or enhancement in different transverse momentum or rapidity regions. Other processes are, however, hardly noticeable because they only provide some redistributions in an already almost statistical distribution of hadrons. It is a matter of "trial and error" to find the relevant ones in this sense.

Finally in section 5 we consider some predictions from the rescattering process.

2 The FRITIOF Model

2.1 The Longitudinal Energy Momentum Transfers

It is a surprising and gratifying fact that the basic FRITIOF model interaction mechanism is obtained in case we consider the encounter between hadronic strings either *as a measuring process* or *as the results of multiple parton interactions.* In both cases we end up with the same final string states, excited due to the possible longitudinal energy transfer into transverse fronts moving forward and backward along the beam direction.

One may question whether a (semiclassical) string dynamical scenario should have any relevance at all in hadronic physics. It is known, [12] that a possible vacuum structure for nonabelian gauge theories is provided by a color superconducting state with gluonic field configurations corresponding to the Cooper pairs in an "ordinary" electro-magnetic superconductor. In case this structure exists as the lowest energy state (which has not been proved) it is a further question whether the state works as a superconductor type I (with breakdown regions like "bags" or transversely extended "flux tubes" as the result) or as a superconductor type II (where the corresponding structures are vortex lines). A dynamical vortex line must have properties very similar to a massless relativistic string.

In this latter case there is in case the magnetic field, $\mathcal{H}$, is taken as the order parameter a Meissner effect in case the field is below a certain (material-dependent) value, $\mathcal{H}_1$. But in the region $\mathcal{H}_1 \leq \mathcal{H} \leq \mathcal{H}_2$ the quantised vortex lines start to penetrate the superconducting state and exhibit a repulsive relative interaction. Above $\mathcal{H}_2$ the field is so strong that the whole region "melts" into a state of the same character as the break-down of a superconductor type I. This "melted" vacuum state is often used as an intuitive picture for a quark-gluon plasma.

The string picture, inherent in the Lund Model, for the color force fields is also strongly supported by the results of the e^+e^--annihilation experiments at LEP as described by the perturbative QCD cascades. Whether one makes use of the "individual parton cascades" typically the ones described by HERWIG in accordance with Webber-Marchesini, [13], or the Dipole Cascade Model (DCM), described by ARIADNE, there are due to the coherence of QCD bremsstrahlung only certain regions of phase space which contain color force fields. If the final state particle distributions are described in terms of the decay of "a chain of clusters" (Webber's method) or by means of the fragmentation of a Lund Model string the results nevertheless become very similar. The results of deep inelastic scattering from EMC to HERA also support this picture.

We start with *the measuring process* and assume that the two hadronic states, impinging upon each other, will lead to some transverse overlap between the strongly Lorentzcontracted states. The two hadrons will approach each other with the original very large lightcone energy momenta P_{+1} and P_{-2} and then the typical overlap "lightcone times" will be $t_{-2} \sim 1/P_{+1}$ and $t_{+1} \sim 1/P_{-2}$. (Note that quantum theory allows the localisation of one of the pairs $(P_\pm, t_\pm)$ simultaneously for each incoming hadronic state). On a short time basis there should be quantum mechanical fluctuations into all the hadronic states with the "right" quantum numbers. Therefore all the hadronic states with a (virtual) lifetime longer than the interaction times will be available and then it should be possible to project into them. The possible final states are then the string states with (p_{+j}, p_{-j}) such that $p_{+2} < P_{+1}$ and $p_{-1} < P_{-2}$. Introducing the momentum transfer $(Q_+, -Q_-)$ from $1 \rightarrow 2$ we obtain the states with $(P_{+1} - Q_+, Q_-)$ and $(Q_+, P_{-2} - Q_-)$ with the requirements that $m^2/P_+ < Q_+ < P_{+1}$ and $m^2/P_+ < Q_- < P_{-2}$.

Despite the Lorentz contraction properties it may well be that the transversely (space) extended fronts "only gradually" meet and define each other. Then a multiple scattering parton scenario is a more relevant description. The surprising result on a stringlike force field is that both situations will lead to the same kind of final state, ie a gradual stretching out of a longitudinal string field (besides internal transverse excitations in the form of bremsstrahlung gluons, cf below).

In case there are multiple parton scatterings a large set of partons from 1, with energy momenta k_{1j} will scatter against another set k_{2j} from 2 with the momentum transfers q_j, such that $\sum q_j = Q$. In case the scatterings are uncorrelated then it is reasonable to expect $\vec{Q}_\perp \simeq 0$ (also "locally") but the longitudinal transfers should be nonvanishing in order to keep the partons on the mass-shell.

Now a string is locally a strongly correlated dynamical object. In case there is a set of longitudinal excitations over some region then the string will be dragged out "piece by piece" using up the energy momentum of the excitations in turn of color ordering along the field. The difference between applying a large momentum transfer $Q_\pm$ at the end of a string moving "forward" with $P_\mp - Q_\mp$ and the application of a set of momentum transfers $q_{\pm j}$ (with $\sum q_{\pm j} = Q_\pm$) over a connected region is small as long as there are no large transverse excitations along the front. In both cases the final state string will (in case it does not break up) have a longitudinal extension in the cms of the order $2W_j/\kappa$ with κ the string constant and with $W_1^2 = (P_+ - Q_+)(Q_-)$ and $W_2^2 = (Q_+)(P_- - Q_-)$. On the other hand the transverse extension will be of the order of m/κ with m the (original) hadronic restmass. This means that the final state in both cases will look very similar to a Lund Model string as used in e^+e^--annihilation reactions and we will consequently treat the strings in the same way with respect to fragmentation.

In FRITIOF the basic dynamics is provided by the longitudinal momentum transfers $Q_\pm$ which are assumed to be distributed in a scaling way:

$$\propto \frac{dQ_+ dQ_-}{Q_+ Q_-} \tag{1}$$

2.2 Transverse Momentum Transfers and Bremsstrahlung

There is further incorporated the possibility that there is a single hard Rutherford scattering between the partons, ie one of the multiple collisions is "hard". We treat it by means of the simulation routines in PYTHIA. Then the final string states will contain these hard excitations, ie one large $k_\perp$ parton in each string. If the parton is a valence constituent the excitation is placed at the ("backward") end-point of the string while for a g it is placed inside the final state string (with the longitudinal transfers according to Eq (1) distributed around it).

The appearance of such an excitation also implies that the longitudinal momentum transfers must increase. Suppose that a parton from hadron 1 (2) with original energy momentum $x_1 P_+$ ($x_2 P_-$) is scattered into the energy-momentum state $(k_{+1}, k_{-1}, \vec{k}_{\perp R})$ ($(k_{+2}, k_{-2}, -\vec{k}_{\perp R})$). Then the lower bound on the variables $(Q_\pm)$ in the distribution in Eq (1) is given by (k_{+2}, k_{-1}) instead of $(m^2/P_\mp)$ in case there is no Rutherford parton scattering. This feature accounts in the FRITIOF model for the so-called "pedestal effect", ie the increased activity in the surroundings of large jets.

In order that a particular Rutherford scattering should be a relevant perturbative contribution it is essential that the possible bremsstrahlung in the hadronic states are less hard, ie corresponds to smaller transverse momenta than the Rutherford $\vec{k}_{\perp R}$. This is incorporated in the FRITIOF Model and in this way it is always the largest transverse momentum excitation (whether from bremsstrahlung or from Rutherford scattering) which governs the remaining features of the state.

The bremsstrahlung spectrum in FRITIOF is given by the ordinary DCM pattern, ie with the coherence condition of color bremsstrahlung incorporated, together with a particular damping condition according to the SRM. An e^+e^--annihilation event in the DCM contains originally a dipole between the produced quark (q, a color-3) and antiquark ($\bar{q}$, a color-$\bar{3}$). The current after the emission of a gluon (g, a color-8) can to a very good approximation be treated as *two independent dipoles*, one between the (qg) and one between the $(g\bar{q})$ in case the gluonic emissions are ordered in transverse momentum size. After a second emission there will be three independent dipoles etc.

The phase space for the gluon emission from a dipole with cms energy W can conveniently be described in terms of the transverse momentum, $k_\perp$, and rapidity, y, as

$$k_\perp \cosh(y) \leq W/2 \quad \text{or approximately} \quad k_\pm = k_\perp \exp(\pm y) < W \tag{2}$$

While the color charges in an e^+e^--annihilation state can be treated as pointlike this is no longer the case for the color charges in hadronic interactions. There are once again two different dynamical pictures which in a dual manner produce the same results in the mean.

In the first picture we may imagine the excited states described above as built out of perturbative ladder graphs with repeated partonic splittings, eg $g_0 \rightarrow g_1 g_1'$, $g_1 \rightarrow g_2 g_2'$ etc (the primed gluons are emitted as real bremsstrahlung while the unprimed correspond to the built up virtual "string" state). Marchesini et al, [14], have shown (cf also for more details Ref [15]) that such splittings can be treated as a set of connected dipoles. For the one described above these dipoles will be between $(g_0 g_1)$, $(g_1 g_1')$, $(g_1 g_2)$, $(g_2 g_2')$ etc.

Therefore such a ladder graph spanned between a parton p_0 and the final end parton p_n is not a single "large" dipole, $(p_0 p_n)$. Thus in FRITIOF there is not a single dipole between the forward, $P_+ - Q_+$, and backward, Q_-, moving fronts but a set of smaller mass emitters. This leads to damping of hard, large $k_\perp$, bremsstrahlung. The resulting pattern turns out to be equivalent, [15], to the one promoted several years ago by the SRM, [5].

The SRM considers the situation when the color charges and the related energy momentum have a transverse extension (like in the FRITIOF "fronts") with a size parameter l. Then in case radiation with a wavelength, λ, smaller than l is emitted from such an "antenna" there will be a damping condition (corresponding to a form factor). In the SRM one assumes that only the fraction $(\lambda/l)^d \equiv (\mu/k_\perp)^d$ of the energy momentum is available, ie that Eq (2) is changed into

$$k_\pm \equiv k_\perp \exp(\pm y) < (\mu/\lambda)^d W \tag{3}$$

There are two parameters, the inverse size μ and the power d, which corresponds to the transverse dimension of the emitter. The parameters have been fitted to experimental data and it is interesting that d is always found to be close to 1, ie like a string. This is also the average behaviour of the dipole chain emissions described above.

The parameter μ depends upon the starting conditions in the connected chain and the experimental fits prefer a value of around 0.6 GeV, ie a very reasonable inverse hadronic size.

In conclusion a single hadronic collision in the FRITIOF Model will lead to a final state containing two (longitudinally) extended string states with some internal excitations corresponding either to a single Rutherford scattered gluon (the largest $k_\perp$) or to gluons emitted in accordance with the DCM and the SRM.

This scenario is extended to hadron-nucleus and nucleus-nucleus collisions by the assumption that the projectile (and target) hadrons may undergo several collisions according to a geometrical picture. This will lead to final states defined by the logarithmic $Q_\pm$ spectrum with the longitudinal momentum transfers increasing (ie after a second collision the hadrons will obtain values of $Q_\pm$ according to Eq (1), with the lower limit defined by the earlier one etc). The "hardest" Rutherford is retained in this multiple collision process and the bremsstrahlung is again performed according to DCM and SRM.

3 The Formation Time and the Initiation of the Rescattering Process

3.1 The Formation Time

The Landau Pomeranchuk formation time concept stems from the following considerations. Consider a charged particle in a QED-based process and ask when it is possible to differ between a state containing solely the charge and the state containing the charge and possible surrounding bremsstrahlung photons. In case we concentrate on a photon with transverse momentum $k_\perp$ and energy E then it is always possible by means of a boost with the γ-factor $E/k_\perp$ to go to a frame where the photon is directed solely transversely. In this frame it is necessary to wait at least the time corresponding to a wave-length, ie $\tau \simeq 1/k_\perp$ before the photon can be observed. From time dilation arguments this means that it will in the original frame take the time $t \simeq (E/k_\perp)\tau = E/k_\perp^2$. Thus the higher the photon energy the longer time it will take to observe the photon.

There is in a string fragmentation scenario a corresponding notion. The proper time to form the final state particles has a distribution with a generally strong peak around the mean. Therefore the particles tend to "come out" along a hyperbola in space time with the proper time τ distributed as

$$\propto \Gamma^a \exp(-b\Gamma) \quad \text{with} \quad \Gamma = \kappa^2\tau^2 \tag{4}$$

ie with the correspondence to the inverse photon transverse momentum above, $<\tau>\simeq 1/\kappa\sqrt{(1+a)/b}$. Here a and b are the Lund Model fragmentation parameters (cf JETSET) and using the ordinary values one finds $<\tau>\simeq 1$ fm/c.

For simplicity we have used a constant "proper formation time", τ_0, the same for all kinds of hadrons, and kept it as a free parameter with a default value 1.5 fm/c. In a moving frame the formation time is then for a hadron of mass m and energy E equal to $E\tau_0/m$.

Bialas and Gyulassy[16] have introduced two formation times for string fragmentation: constituent and yoyo-formation time, τ_c and τ_y, respectively. τ_c is the time when the string breaks, i.e. new constituents are created; τ_y is the time when the 'yoyo-state' is formed. In RQMD rescattering occurs for times $\tau_c < t < \tau_y$ between constituent (di)quarks and hadrons; MCFM includes hadron-hadron rescattering, i.e. $t > \tau_y$, while QGSM contains both diquark-hadron and hadron-hadron rescattering. In LUCIAE we only consider rescattering after the constituent (di)quarks are hadronized.

3.2 The Initiation in Space-Time

We will assume that from the formation time and onwards a particular final state hadron will be moving "outwards" and therefore be available for rescattering and so will the the "spectators" (ie those nucleons which did not participate in the high energy encounter). We also make use of classical trajectories for each one of the produced hadrons assuming that the produced particles are initially randomly placed at the formation time in space inside the (classical) overlap region of the participant and the nucleus. The "spectator" nucleons are likewise randomly distributed inside the non-interacting region and provided with a thermal motion in accordance with a Boltzman distribution. We require as always that that there is a minimum distance between such spectators ("the hard intranuclear core potential") of 0.5 fm.

3.3 The Initiation in Momentum Space

The produced particles from the fragmentation have already had their four-momentum calculated according to the Lund Fragmentation Model. For the projectile spectator nucleons, it is reasonable to assume that they share the remaining longitudinal momentum of the projectile, ie the one not used up to produce hadrons. The transverse momentum of the spectators are sampled according to the two dimensional Gaussian distribution

$$f(p_t)dp_t = Cp_t \exp[-\frac{p_t^2}{< p_t^2 >}]dp_t. \tag{5}$$

Here $\sqrt{< p_t^2 >}$ is taken to be 200 MeV. The transverse momentum of the last projectile spectator nucleon should be decided by transverse momentum conservation so that the energy-momentum conservation is guaranteed.

3.4 The Classical Motion of The Particles and The Collision Times

The hadrons are treated as classical, point-like particles, which move along straight-line trajectories between two consecutive collisions

$$\vec{r_i} = \vec{R_i} + \vec{\beta_i}(t - T), \tag{6}$$

where $\vec{R_i}$ and T is the four-coordinate of the i-th particle at the time of the last collision.

The particles produced from inelastic scattering would also interact with other hadrons. In order to perform the collisions in a consistent way it is necessary to introduce a time ordering procedure, i.e. for deciding which pair will collide next we have to calculate the collision times for all pairs of particles and then chose the pair with miminal collision time. In doing so, we have chosen the cms frame of the two colliding particles to calculate the collision times. Two particles will collide if their distance approaches d_{min} with

$$d_{min} \leq \sqrt{\frac{\sigma_{tot}}{\pi}}, \tag{7}$$

where σ_{tot} is the total cross section in fm^2. Since the minimum distance depends on the reference frame it is necessary to view this problem in an inertia frame, where the distance of the closest approach will be perpendicular to the momentum of both particles, [17]. If the particles i and j are chosen as an example, their equations of motion are

$$\vec{r_i^*} = \vec{R_i^*} + \vec{\beta_i^*}(t^* - T_i^*) \quad \text{and} \quad \vec{r_j^*} = \vec{R_j^*} + \vec{\beta_j^*}(t^* - T_j^*). \tag{8}$$

Thus one may calculate the relative distance squared between the particle i and j, $d^2(t^*)$. The minimum distance, d^2_{min1}, in the orbits and also the collision time is obtained from

$$\frac{\partial(d^2(t^*))}{\partial t^*} = 0 \quad \text{ie} \quad t_{ij}^* = \frac{[\Delta\vec{R}^*\Delta\vec{\beta}^* + \Delta\vec{\beta}^*(\vec{\beta}_j^* T_j^* - \vec{\beta}_i^* T_i^*)]}{(\Delta\vec{\beta}^*)^2} \tag{9}$$

$$\Delta\vec{R}^* = \vec{R}_j^* - \vec{R}_i^* \quad \text{and} \quad \Delta\vec{\beta}^* = \vec{\beta}_j^* - \vec{\beta}_i^*. \tag{10}$$

The d^2_{min1} must satisfy the Eq (7) and as the collisions must be causal the collision time must fulfil

$$t_{ij}^* \geq Max(T_i^*, T_j^*). \tag{11}$$

After the collision times of all pairs have been calculated in their own cms one has to transfer them back to the lab system.

4 The Treatment of the Particle-Particle Collisions

4.1 The Elastic Scatterings

A particle-particle collision is always performed in the joint cms, for both elastic and inelastic scatterings. If the total and the elastic cross section satisfies

$$\frac{\sigma_{el}}{\sigma_{tot}} \geq \xi \tag{12}$$

where ξ is a random number, then the particles will be elastically scattered or else the collision will be considered as inelastic, cf the next subsection. The distribution of the momentum transfer, t, will for elastic scattering be taken as, [18]

$$\begin{aligned} \frac{d\sigma}{dt} &\sim \exp(Bt), & (13)\\ B &= \frac{\epsilon^6}{1+\epsilon^6}A, & (14)\\ \epsilon &= 3.65(\sqrt{s}-m_i-m_j), & (15)\\ A &= Min[10.3,(1.12<p_t>)^{-2}], & (16) \end{aligned}$$

where $< p_t >$ is the average transverse momentum of the rescattered particles. Thus t is calculated by means of the random number ξ as

$$t = \frac{1}{B}\ln[\xi + (1-\xi)\exp(Bt_0)] \quad \text{with} \quad t_0 = -4(p_i^*)^2. \tag{17}$$

The polar angle of the scattering is then related to t by

$$t = -2(p_i^*)^2(1-\cos(\theta^*)). \tag{18}$$

and the azimuthal angle will be isotropically distributed.

4.2 The Inelastic Collisions

As it is impossible to include all inelastic channels in the program we have chosen to consider only those reactions which we have found to give noticeable effects in the final state spectra. The following inelastic reactions are included in LUCIAE2.0:

- 1) $\pi + \pi \rightarrow \overline{K} + K$

- 2) $\pi + N \rightarrow \Delta + \pi$
- 3) $\pi + N \rightarrow \rho + N$
- 4) $N + N \rightarrow \Delta + N$
- 5) $\pi + N \rightarrow K + Y$
- 6) $\pi + \overline{N} \rightarrow \overline{K} + \overline{Y}$
- 7) $\overline{K} + N \rightarrow \pi + Y$
- 8) $K + \overline{N} \rightarrow \pi + \overline{Y}$
- 9) $K + \overline{N} \rightarrow \overline{K} + \bar{\Xi}$
- 10) $\overline{K} + N \rightarrow K + \Xi$

where the hyperons are $Y = \Lambda$ or Σ. Another possible reaction reaction, $N + N \rightarrow N + Y + K$, plays almost no role due to the smallness of the available phase space and the ensuing rate,[19].

The relative probabilities for the different channels in eg (πN)-scattering, (the reactions 2,3 and 5 above) is used to determine the outcome of the inelastic encounter. As the reactions introduced above do not make up the full inelastic cross section, the remainder is again treated as elastic encounters.

We will for simplicity assume that the total, elastic and inelastic cross sections for NN, πN, KN and $\pi\pi$ interactions are constants and we will use the following values for them: $\sigma_{tot}^{NN} = 40$ mb, $\sigma_{tot}^{\pi N} = 25$ mb $\sigma_{tot}^{KN} = 35$ mb and $\sigma_{tot}^{\pi\pi} = 10$mb. The ratio of the inelastic to the total cross section will be taken as $0.75 \sim 0.85$. Further the cross section for $\pi\pi \rightarrow KK$ is conventionally taken to be 3.0 mb.

An isospin averaged formula parametrised in Ref [19] is used for the cross section of the reaction $\pi + N \rightarrow K + Y$. The cross section for the $\overline{K}N$ induced strangeness exchange reactions is assumed to be equal to ten times the corresponding cross section for the πN induced strangeness production reactions, [19]. Finally the cross section for the reactions $\pi\overline{N}$ and $K\overline{N}$ are assumed to be equal to the corresponding cross sections for the reactions πN and $\overline{K}N$ interactions, respectively.

The cross sections of the inelastic reactions given by the isospin averaged parameterization formulas of Ref.[19] for the $\pi + N \rightarrow K + Y$ decrease exponentially with the CMS energy of the two colliding particles . But we know that the total inelastic cross sections of the πN are approximately energy-independent, which means that more inelastic channels would occur like $\pi^- + p \rightarrow K^{*0} + \Lambda \rightarrow K + \pi + \Lambda$ and $\pi^- + p$

$\rightarrow K^{*0} + \Sigma^0 \rightarrow K + \pi + \Sigma^0$ etc., when the CMS energy of the two colliding particles is increasing. In some sense the reactions we listed above should be looked upon as 'representative channels' of certain types of reactions. Therefore instead of applying energy-dependent inelastic cross section, we could alternatively give a constant 'effective cross section' to the reactions $\pi + N \rightarrow K + Y$.

We always assume that the highest isospin state contributes to the inelastic cross sections in order to calculate the relative cross sections for the different isospin channels. As an example, for the reaction $\pi + N \rightarrow \Delta + \pi$ we assume that the isospin $I = 3/2$ state is dominant. By giving a relative cross section to each inelastic channel the isospin conservation is guaranteed in the rescattering process.

As usual, two body final state, i.e. the energy and momentum of the scattered particles of the inelastic reactions above can be calculated from two-body kinematics, [20], in the cms of the colliding particles, i.e.

$$E_i^* = \frac{s - m_j^2 + m_i^2}{2\sqrt{s}}, \tag{19}$$

$$|\vec{p}_i^*| = \frac{\sqrt{(s - (m_i + m_j)^2)(s - (m_i - m_j)^2)}}{2\sqrt{s}}. \tag{20}$$

The orientation of the three momentum is isotropically sampled in 4π for NN and $\pi\pi$ collisions as suggested in, [18], but for the rescattering between a meson and a baryon we assume that the final state baryon moves along the direction of the incoming baryon in the cms of the colliding particles.

We will finally assume that all the unstable particles produced through the rescattering processes will survive until the end of the heavy-ion collision process.

5 Results and Their Comparisons with Data

5.1 Rapidity Distributions

The easiest way to see the rescattering effect of the final state particles is the rapidity distributions. It has been known from NA35 O+Au collisions at CERN, [21] [22] that the peaks of the rapidity distributions shift somewhat backwards to lower rapidities when comparing with model calculations based on assumption that nucleus-nucleus collisions are made of independent superposition of nucleon-nucleon collisions, which indicates additional particle production in secondary collisions between produced particles and spectators. The effect will also increase the stopping power of the collisions.

In order to see this rescattering effect we plot in Fig.1 the pseudorapidity distribution of charged particles in 200 GeV/c S+Au collisions for three centralities based on both LUCIAE and FRITIOF calculations. The predictions are compared with data from WA80 Collaboration in which ZDC (the zero degree calorimeter) is used to decide the centralities of events, [23]. It is clear that the pseudorapidity distributions shift towards the target fragmentation region due to the rescattering. The more central collisions are, the greater the rescattering effect is.

5.2 Strangeness Production

Another example to show the rescattering effect is the strangeness production in relativistic pA and AA collisions.

It has been a decade since strangeness enhancement was put forward as a possible signature for the formation of a QGP state in a relativistic heavy-ion collision. However, from the discussion in the previous section it is clear that the rescattering of the final state particles would also cause strangeness enhancement. The main reactions that contribute to the production of K^+ and K^- are $\pi + \pi \rightarrow \overline{K} + K$ because of the π dominance in final state. We can immediately see that K^+ will be enhanced with respect to K^- after the rescattering since K^- would be absorbed by the nuclear matter through $\overline{K} + N \rightarrow \pi + Y$ and $\overline{K} + N \rightarrow K + \Xi$ while K^+ would be produced through $\pi + N \rightarrow K + Y$ and $\overline{K} + N \rightarrow K + \Xi$. The reaction $\pi + \overline{N} \rightarrow \overline{K} + \overline{Y}$, $K + \overline{N} \rightarrow \overline{K} + \overline{\Xi}$ and $K + \overline{N} \rightarrow \pi + \overline{Y}$ will hardly affect the amount of K^+ and K^- since the reaction rates of the three reactions are very low due to the poor abundance of $\overline{N}$. This paper does not intend to study the K/π ratios in more detail for it has already been discussed in an earlier paper, [24]. We only list the ratios from FRITIOF and LUCIAE calculations in the full phase space in Table 1.

The production of the neutral strange particles (Λ, $\overline{\Lambda}$, K_s^0) has been studied by many experimental groups at different energies for different reactions, [25] [26] [27]. In paper , [26] the production of the $\Lambda, \overline{\Lambda}$ and K_s^0 is studied by the NA35 Collaboration in full rapidity space for the reactions pp, pA and AA and the multiplicity ratios of the neutral strange particles to negatively charged particles are found to increase from the pp, pA to AA.

In Table 1 we list our calculations of the multiplicities of $\Lambda, \overline{\Lambda}$ and K_s^0 from LUCIAE and FRITIOF for reactions pp, p-S, S-S, S-Ag and S-Pb at 200 AGeV/c. The calculations for the multilicity ratios of the neutral strange particles to negatively charged particles and the K/π ratios are also included. Comparisons with experimental data are given if correspondent data are available. Note that the Λ and $\overline{\Lambda}$ here include the decay products of Ξ and $\overline{\Xi}$.

We see from Table 1 that FRITIOF predicts no increase of the neutral strange particles over negatively charged particles from pp to AA collisions, but LUCIAE does show a steady increase of the strangeness production, which reveals the importance of the rescattering effect. FRITIOF predicts again no considerable increase in the K^+/π^+, the increase from LUCIAE calculation is thus due to the rescattering effect. Both FRITIOF and LUCIAE predict an approximately constant K^-/π^-.

Another way to investigate the strangeness production in the high energy AA collisions is to study the dependence of the strangeness production on impact parameter. When one goes from grazing collisions to central collisions in the AA collisions, the energy density and the baryon density increase as they do from pp to AA collisions. We notice from Table 1 that the increase of the strangeness production shows a tendency of saturation when the multiplicity of negatively charged particle reaches about 100 at S-S collisions. This may correspond to the 'saturation' phenomenon of the strangeness production seen in S-Pb collisions at 200 AGeV/c, [25]. Fig.2 show our calculations for Λ from both FRITIOF and LUCIAE together with experimental data of paper, [25] for S-Pb collisions at 200 AGeV/c. The differences between LUCIAE and FRITIOF prediction are clearly seen.

Acknowledgments

This research is supported in part by the EU Programme "Human Capital and Mobility", Network "Physics at High Energy Colliders", contract CHRX-CT93-0357 (DG 12 COMA).

References

[1] B. Andersson, G. Gustafson and B. Nilsson-Almqvist, "A High Energy String Dynamics Model for Hadronic Interactions", LU−TP−87−6.

[2] B. Andersson, G. Gustafson and H. Pi, Z. Phys. C57 (1993) 485.

[3] T. Sjöstrand, "A Manual to The Lund Monte Carlo for Jet Fragmentation and e^+e^- Physics: JETSET version 7.3", available upon request to the author.

[4] G. Gustafson, Phys. Lett. 175B (1986) 453; G. Gustafson and U. Pettersson, Nucl. Phys. B306 (1988) 746.

[5] B. Andersson et al. Z. Phys. C43 (1989) 625.

[6] H. -U. Bengtsson and T. Sjöstrand, Comput. Phys. Commun. 46 (1987) 43.

[7] L. Lönnblad, "`ARIADNE version 4`, A Program for Simulation of QCD Cascades implementing the Colour Dipole Model", *DESY* 92-046.

[8] J. Ranft, S. Ritter, Z. Phys. C20 (1983) 347; J. Ranft, S. Ritter, Z. Phys. C27 (1985) 569.

[9] J. Ranft, Z. Phys. C43 (1989) 439.

[10] H. Sorge, H. Stöcker and W. Greiner, Nucl. Phys. A498 (1989) 567c; H. Sorge et al., Z. Phys. C47 (1990) 629.

[11] N. S. Amelin et. al., Phys. Rev. C44 (1991) 1541.

[12] H.B. Nielsen and P. Olesen, Nucl. Phys. B61 (1973) 45.

[13] B.R. Webber, Nucl. Phys. B238 (1984) 492; G. Marchesini and B.R. Webber, Nucl. Phys. B238 (1984) 1.

[14] S. Catani, F. Fiorani and G. Marchesini, Phys. Lett. B234 (1990) 339; Nucl. Phys. B336 (1990) 18 .

[15] B. Andersson, G. Gustafson and J. Samuelsson, to be published.

[16] A. Bialas and M. Gyulassy, Nucl. Phys. B291 (1987) 793.

[17] S. P. Sorensen, private communication.

[18] J. Cugnon, T. Mizutani, and J. Vandermeulen, Nucl. Phys., A352, (1981) 505.

[19] P. Koch, B. Müller and J. Rafeiski, Phys. Rep. 142, (1986) 167.

[20] Particle data group, Phys. Lett., B239, (1990).

[21] NA35 Collaboration, H. Stroebele, et al., Z. Phys. C38 (1988) 89

[22] HELIOS Collaboration, T. Akesson, et al., Nucl. Phys. B353, (1991) 1 .

[23] R. Albrecht et al., Z. Phys. C55 (1992) 539-548.

[24] Sa Ben-Hao et al. Phys. Rev. C 48 (1993) 2995.

[25] NA36 Collaboration, E. Andersen, et al., Phys. Lett., B316 (1993) 603.

[26] NA35 Collaboration, J. Bartke, et al., Z. Phys. C48 (1990) 191-200.

[27] NA35 Collaboration, T. Alber, et al., Z. Phys. C64 (1994) 195-207.

[28] NA35 Collaboration, M. Gazdzicki, Nuclear Physics A566 (1994) 503c-506c.

Table 1.

Reaction		p + p	p + S 'min.bias'	S + S 'central'	S + Ag 'central'	S + Pb 'central'
$< h^- >$	FRITIOF	2.87	5.0	105	160	193
	LUCIAE	2.87	5.2	107	167	206
	DATA	2.85 ± 0.03	5.7 ± 0.2	98 ± 3	170 ± 8	
$< \Lambda >$	FRITIOF	0.162	0.25	4.78	7.47	8.91
	LUCIAE	0.166	0.37	6.63	12.30	16.24
	DATA	0.095 ± 0.010	0.28 ± 0.03	9.4 ± 1.0	15.2 ± 1.2	
$< \overline{\Lambda} >$	FRITIOF	0.025	0.045	0.89	1.33	1.69
	LUCIAE	0.025	0.045	1.22	2.10	2.55
	DATA	0.013 ± 0.005	0.049 ± 0.006	2.2 ± 0.4	2.6 ± 0.3	
$< K_s^0 >$	FRITIOF	0.22	0.37	7.56	11.74	14.13
	LUCIAE	0.22	0.38	8.88	14.5	17.94
	DATA	0.17 ± 0.01	0.38 ± 0.05	10.5 ± 1.7	15.5 ± 1.5	
$\frac{<\Lambda>}{<h^->}$	FRITIOF	0.056	0.050	0.047	0.047	0.046
	LUCIAE	0.058	0.071	0.062	0.074	0.079
	DATA	0.033 ± 0.004	0.049 ± 0.006	0.096 ± 0.012	0.089 ± 0.009	
$\frac{<\overline{\Lambda}>}{<h^->}$	FRITIOF	0.0088	0.0090	0.0085	0.0083	0.0088
	LUCIAE	0.0088	0.0086	0.011	0.013	0.012
	DATA	0.0046 ± 0.0014	0.0086 ± 0.0011	0.022 ± 0.004	0.015 ± 0.002	
$\frac{<K_s^0>}{<h^->}$	FRITIOF	0.077	0.074	0.072	0.073	0.073
	LUCIAE	0.078	0.073	0.083	0.087	0.087
	DATA	0.060 ± 0.004	0.067 ± 0.001	0.11 ± 0.019	0.091 ± 0.011	
$\frac{<K^+>}{<\pi^+>}$	FRITIOF	0.088	0.094	0.098	0.098	0.097
	LUCIAE	0.089	0.10	0.12	0.13	0.13
	DATA	0.08 ± 0.01		0.137 ± 0.008		
$\frac{<K^->}{<\pi^->}$	FRITIOF	0.075	0.072	0.071	0.070	0.070
	LUCIAE	0.076	0.058	0.076	0.073	0.070
	DATA	0.06 ± 0.01		0.076 ± 0.005		

Table 1: The multiplicities of $\Lambda, \overline{\Lambda}$ and K_s^0 from LUCIAE and FRITIOF calculations for reactions pp, p-S, S-S, S-Ag and S-Pb at 200 AGeV/c and the multiplicities ratios of the neutral strange particles to negatively charged particles together with their comparisons with experimental data. The K/π ratios are also included in the table. Data are from, [27] [28].

Figure Captions

Fig.1: Pseudorapidity distribution of charged particles for S+Au collisions for three different centrality cuts, ($\times$)0−20%, ($\diamond$)45%−55% and ($\square$)75%−85% of the beam energy measured at zero degree. The solid histograms are LUCIAE calculation and the dished histograms are FRITIOF calculation. Data are from [23].

Fig.2: Λ production as a function of negative multiplicity for S-Pb collisions at 200 GeV/c per nucleon. The solid lines are prediction of LUCIAE and the dashed lines are that of FRITIOF. The data points are from, [25].

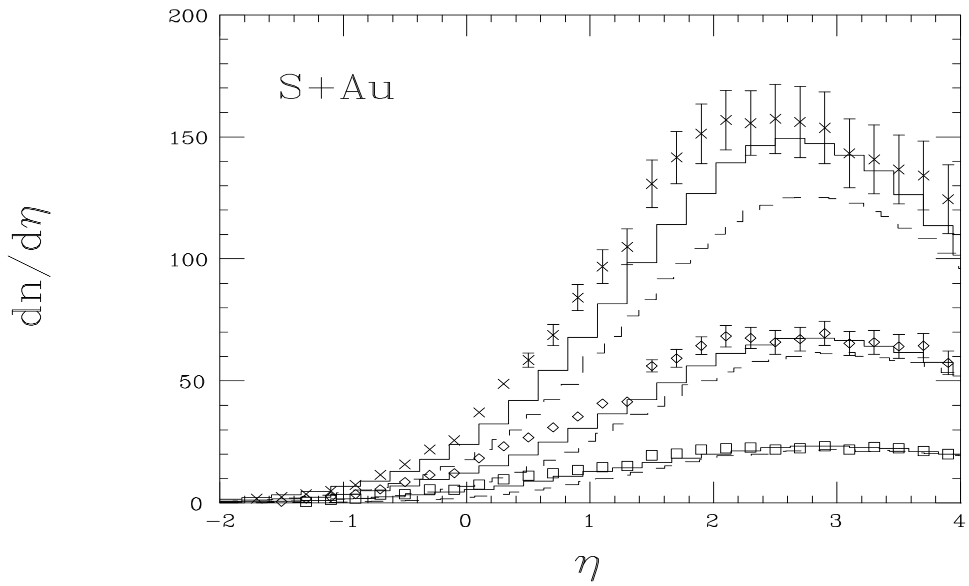

S+Au
dn/dη
η
200
150
100
50
0
−2
−1
0
1
2
3
4

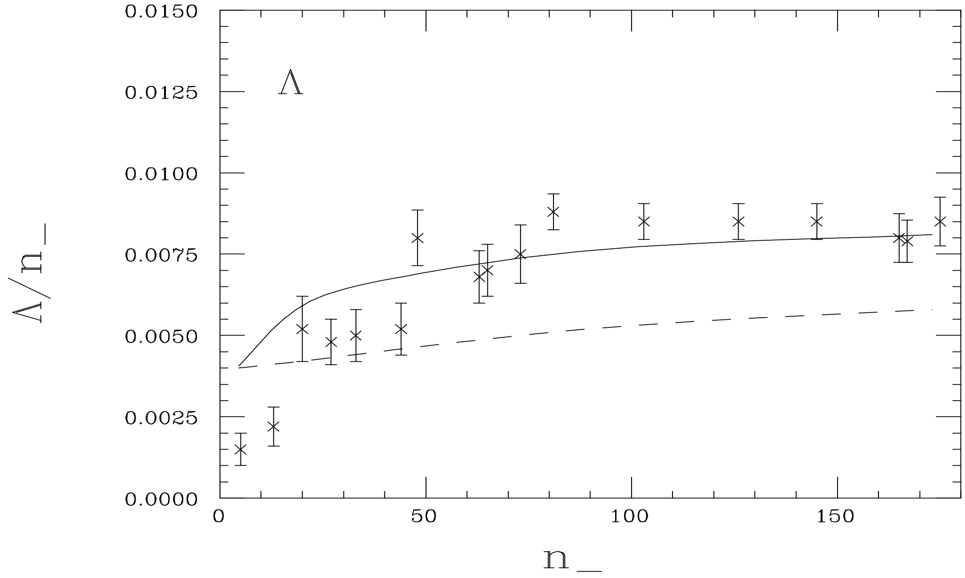

0.0150
0.0125
0.0100
0.0075
0.0050
0.0025
0.0000
0
50
100
150
Λ
Λ/n_
n_